CPE-73

# Effect of Injection Position on Throttle Body Injection Mixer for Compressed Natural Gas Motorcycle

Yvonne, S. H. Chang[1], Zukefli Yaacob[2], Rahmat Mohsin[3] and Zulkifli Abd Majid[2]

[2]Gas Engineering Department
[3]Gas Technology Centre (GASTEG)
Universiti Teknologi Malaysia, 81310 Skudai, Johor, Malaysia.
Tel: +60-12-7702410, E-mail: [1]yvonne_csh@yahoo.com

## Abstract

*A good gaseous mixer must be able to prepare a homogeneous mixing of air and fuel at a specific air-fuel ratio prior to entering the engine in order to avoid low fuel efficiency and high exhaust emissions. Thus, effect of injection position on the mixing in Throttle Body Injection Mixer (TBIM) for a compressed natural gas (CNG) motorcycle was investigated in this work through Computational Fluid Dynamics (CFD) modelling. The aim of CFD modelling was to study the effect of various injection positions on the mixing in TBIM, which otherwise was not available visually through experimental work. The optimum injection position throughout the case studies was also investigated in this work. CFD results revealed a significant effect of various injection positions on the hydrodynamics of air and fuel in TBIM. Injection position is therefore a fundamental parameter for the mixing in TBIM.*

**Keywords:** Injection position, Throttle Body Injection Mixer (TBIM), Computational Fluid Dynamics (CFD)

## Introduction

Although the overall demand for conventional motor gasoline and gas-oils will continue to grow, the use of alternative fuels must be considered because of the benefits of energy security and clean emissions. Recently, natural gas has been recognized as a promising alternative fuel for internal combustion engines and natural gas vehicles (NGVs) may come into wider use.

Natural gas may be used in the form of compressed gas or cryogenic liquid [1, 2, 3]. In this research, natural gas in the form of compressed gas, called compressed natural gas (CNG) was utilized. Even though CNG is not a panacea for air pollution problems, it has been remarked that CNG has considerable potential as a cleaner fuel for internal combustion engines as compared to the conventional fuels. Extremely low photochemical reactivity, low carbon dioxide ($CO_2$) and nitrogen oxide ($NO_x$) emissions, as well as zero evaporative and particulate emissions are some of the distinct benefits of CNG as a vehicular fuel [3, 4, 5, 6, 7]. In addition, owing to its gaseous form, CNG does not need to be vaporized. This implies that fuel enrichment is not required during cold starting or transient operating conditions. Hence, the elimination of cold and transient enrichments has a tendency to reduce both cold-start and low-temperature emissions, leading to a substantial reduction of carbon monoxide (CO) and unburned hydrocarbon (UHC) emissions. More advantages of CNG were discussed in [2, 4]

Nevertheless, poor mixing of air and fuel in the mixer prior to entering the engine is one of the dilemmas of CNG engines nowadays. Premixing of air and fuel in the mixer is said to be inadequate because it adversely influences the engine combustion, which would reduce its power output and increase its pollutant emissions [8, 9]. Furuyama and Xu (1998) conducted a study on the mixing phenomenon of air and fuel in a venturi-type mixer for CNG engines [9]. In their study, the hydrodynamics of air and fuel in the mixer was visualized through Schlieren method. They claimed that the poor mixing of air and fuel was mainly attributed to the throttle transient and the design criteria of fuel nozzle. In addition, an injection-type mixer proposed by Chin (2004) for CNG engines, namely TBIM also exhibited a poor mixing of air and fuel through CFD modelling [10]. It is evident that this subject has not had sufficient study in the past [11] and further research is necessary. Thus, the objective of this work is to investigate the effect of various injection positions on the air-fuel mixing in TBIM for a four-stroke, single-cylinder CNG powered motorcycle with 111cc in capacity. The optimum injection position for a wide range of engine operating conditions would also be determined.

## Justification of Research

To allow clean and stable engine running, the homogeneity of air-fuel mixture prior to entering the engine is of paramount imperative [12]. One of the main problems of inhomogeneous mixing in a mixer is due to the inadequate distribution of mixing energy. However, a simple change in the injection position can normally alter the energy distribution, and thus improve the mixing [13]. Therefore, in order to attain an adequate distribution of mixing energy in TBIM, the effect of injection position was investigated in this work. Figure 1 shows the three different injection positions studied in this research. They are 35 mm, 55 mm and 70 mm away from throttle valve along the x-axis on plane-xy. During the investigation, other parameters such as injection inclination angle, injection frequency and duration of injection time were set as follows:

Injection inclination angle = 90° to throttle bore centre
Injection frequency = 1-injection/engine cycle
Duration of injection time = 80% of 1-stroke time

## Governing Equations and Numerical Solution

The mass conservation equation for an incompressible fluid is

$$\frac{\partial u}{\partial x}+\frac{\partial v}{\partial y}+\frac{\partial w}{\partial z}=0 \qquad (1)$$

This term describes the net flow of mass out of a fluid element across its boundaries [14, 15, 16].

For a turbulent flow, the velocity at any point is taken as the sum of the mean ($\bar{u}_i$) and fluctuating ($u_i'$) components [14, 15, 16]

$$u_i = \bar{u}_i + u_i' \qquad (2)$$

The suffix notation, i represents the iteration of flow directions (i.e. x-, y- or z-direction). Substituting expression of this form into the instantaneous momentum equations yields the ensemble-averaged (mean) momentum equation (Fluent Inc.)

$$\frac{\partial}{\partial x_j}(\rho u_i u_j)=-\frac{\partial P}{\partial x_i}+\frac{\partial}{\partial x_j}\left\{\left[\mu\left(\frac{\partial u_i}{\partial x_j}+\frac{\partial u_j}{\partial x_i}\right)\right]-\frac{2}{3}\mu\frac{\partial u_j}{\partial x_j}\right\}+\frac{\partial}{\partial x_j}\left(-\rho\overline{u_i' u_j'}\right) \qquad (3)$$

where the suffix notation, j represents all the flow directions (i.e. x-, y- and z-direction). The second order tensor of "Reynolds stresses" or $\left(-\rho\overline{u_i' u_j'}\right)$ in Equation 3 is varied with different turbulent models used.

For RNG κ-ε model, it is modelled using the Boussinesq hypothesis [17]. The Reynolds stresses is linked to the mean velocity gradients via

$$\left(\rho\overline{u_i' u_j'}\right)=\frac{2}{3}\left(\rho\kappa+\mu_t\frac{\partial u_i}{\partial x_i}\right)\delta_{ij}-\mu_t\left(\frac{\partial u_i}{\partial x_j}+\frac{\partial u_j}{\partial x_i}\right) \qquad (4)$$

where κ = turbulent kinetic energy, ε = dissipation rate of turbulent kinetic energy and $\mu_t$ = turbulent viscosity.

The $\mu_t$ is computed from the functional form

$$\mu_t=\mu_{t0}f\left(\alpha_s,\Omega,\frac{\kappa}{\varepsilon}\right) \qquad (5)$$

where

$\mu_{t0}$ = $0.0845\rho\frac{\kappa^2}{\varepsilon}$

$\Omega$ = characteristic swirl number (evaluated within FLUENT program)

$\alpha_s$ = swirl constant (swirl-dominated or mildly swirling)

The κ and ε are determined by numerical integration of the system of differential equations

$$\frac{\partial}{\partial x_i}(\rho u_i\kappa)=\frac{\partial}{\partial x_i}\left(\alpha_\kappa\mu_t\frac{\partial\kappa}{\partial x_i}\right)+G_\kappa-\rho\varepsilon \qquad (6)$$

$$\frac{\partial}{\partial x_i}(\rho u_i\varepsilon)=\frac{\partial}{\partial x_i}\left(\alpha_\varepsilon\mu_t\frac{\partial\varepsilon}{\partial x_i}\right)+C_{1\varepsilon}G_\kappa\frac{\varepsilon}{\kappa}-C_{2\varepsilon}\rho\frac{\varepsilon^2}{\kappa}-R_\varepsilon \qquad (7)$$

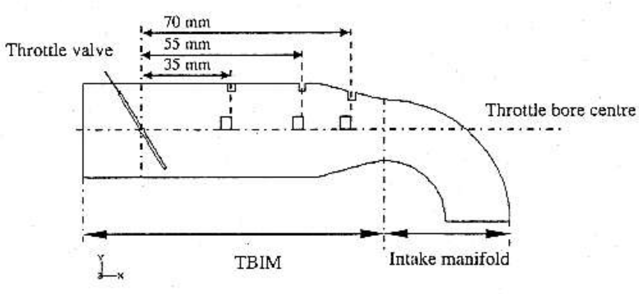


**Figure 1 Three different injection positions studied in this research**

The term $G_\kappa$ (Equations 6 and 7) represents the generation of κ due to the mean velocity gradients, given by (FLUENT Inc, 2001)

$$G_\kappa = -\rho\overline{u_i' u_j'}\frac{\partial u_j}{\partial x_i} \tag{8}$$

or, consistent with the Boussinesq hypothesis (FLUENT Inc, 2001)

$$G_\kappa = \mu_t\left(\frac{\partial u_i}{\partial x_j} + \frac{\partial u_j}{\partial x_i}\right)\frac{\partial u_j}{\partial x_i} \tag{9}$$

The effects of rapid strain and streamline curvature is given by the last term, $R_\varepsilon$ in Equation 7, where (FLUENT Inc, 2001)

$$R_\varepsilon = \frac{0.0845\rho\eta^3\left(1-\dfrac{\eta}{4.38}\right)}{1+0.012\eta^3}\frac{\varepsilon^2}{\kappa} \tag{10}$$

and

$\eta \quad = \quad S\dfrac{\kappa}{\varepsilon}$

$S \quad = \quad$ modulus of the mean rate-of-strain tensor $\left(\sqrt{2S_{ij}S_{ij}}\right)$

$S_{ij} \quad = \quad$ mean strain rate, $\left[\dfrac{1}{2}\left(\dfrac{\partial u_i}{\partial x_j} + \dfrac{\partial u_j}{\partial x_i}\right)\right]$

For a high Reynolds number of flow, the values of the inverse Prandtl numbers for κ and ε $(\alpha_\kappa \text{ and } \alpha_\varepsilon)$ in Equations 6 and 7 are approximately 1.393.

The coefficients $C_{1\varepsilon}$ and $C_{2\varepsilon}$ (Equations 6 and 7) are empirical constants having the following values:

$$C_{1\varepsilon} = 1.42 \quad \text{and} \quad C_{2\varepsilon} = 1.68$$

## Results and Discussion

### Effect of Various Injection Positions

The mixing homogeneity ($H_m$) and air-fuel ratio ($A/F_m$) were two major concerns in determining the effect of various injection positions on the mixing in TBIM and intake manifold through CFD modelling. The former one was defined as the ability to mix with a uniform mass fraction of methane ($M_{ch4}$), while the latter one referred to the ability to mix with a $M_{ch4}$ close to the stoichiometric one in TBIM and intake manifold.

To justify the $H_m$ more effectively, the quality of $H_m$ had been standardized and graded according to the number of contours of $M_{ch4}$ in the mixing region. The best $H_m$, i.e. Grade A, was exhibited by merely one contour of $M_{ch4}$. However, if it happened to have two contours of $M_{ch4}$ instead of one, Grade B would be considered. As for Grade C, it was signified by a total of three contours of $M_{ch4}$ in the mixing region concerned. Finally, the worst $H_m$, which had four or more contours of $M_{ch4}$ in the mixing region concerned, was represented by Grade D.

On the other hand, the $A/F_m$ was investigated through the histograms of $M_{ch4}$. During the investigation, $M_{ch4}$ with the highest frequency ($M_{hf}$) was retrieved from each histogram (Figure 2). The closer the $M_{hf}$ to the stoichiometric $M_{ch4}$, the better the $A/F_m$ obtained and vice versa. The targeted stoichiometric $M_{ch4}$ in this research was calculated as follows:

Stoichiometric air-fuel ratio = 17.3 : 1

Thus, the stoichiometric $M_{ch4}$ = 1/18.3 = **0.0546**

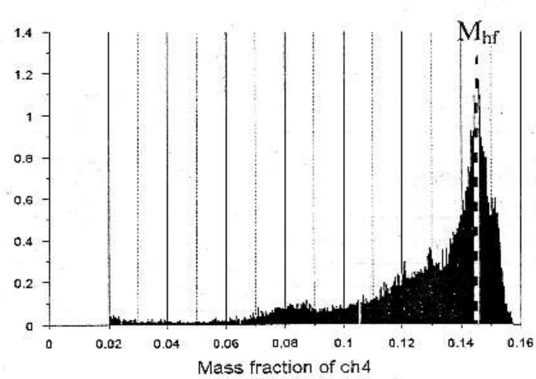


**Figure 2** **Histogram of $M_{ch4}$ used to determine $M_{hf}$**

Table 1 reveals the effect of various injection positions on the $H_m$ and $M_{hf}$ in TBIM and intake manifold. The four different injection positions studied were 35mm (tp35), 55mm (tp55) and 70mm (tp70) away from throttle valve along x-axis on plane-xy.

On the whole, the $H_m$ was improved dramatically when the injector position was changed from tp35 (controlled case) to either tp55 or tp70 for all the engine speeds. The $H_m$ obtained at both tp55 and tp70 happened to be exactly the same throughout the engine speeds. Unlike the $H_m$, the $M_{hf}$ did not show any remarkable improvement with various injection positions. In most cases, the $M_{hf}$ obtained were much higher than the stoichiometric $M_{ch4}$, and it increased with the distance of injector from throttle valve. The higher $M_{hf}$ found at tp55 and tp70 than those at tp35 for each engine speed, except for tp55 at 7200rpm, implied an inferior distribution of methane when positioning the injector closer to the intake manifold. However, these $M_{hf}$ were found to decrease with increasing engine speeds for a particular injection position, except for tp55 at 1260rpm. In short, a varying injection position was incapable to improve the $A/F_m$ but $H_m$ in TBIM and intake manifold.

The improvement of $H_m$ by a varying injection position was closely related to the distribution of mixing energy in TBIM and intake manifold. In fact, inappropriate positioning of injection in a mixer normally leads to an insufficient distribution of mixing energy, which is a recurring source of poor mixing in most industrial practices [13]. A simple alteration of injection position can always change the mixing energy distribution and thus, enhance the mixing [13]. In this research, the $H_m$ in TBIM and intake manifold was found to improve when the injector was switched from tp35 to either tp55 or tp70 for all the engine speeds. For tp55 and tp70, the injector was located close to or at the reducer where the velocity increased and the pressure decreased [18]. Consequently, a high-velocity flow was generated in the reducer. This high velocity of flow in the reducer provided an additional force on the distribution of the mixing energy. This extra force, coupled with that from the injection momentum, leaded to an enhancement of $H_m$ for tp55 and tp70.

**Effect of Various Injection Positions throughout the Case Studies**

Table 2 reveals the effect of various injection positions on the $H_m$ and $M_{hf}$ throughout the case studies. The same injection positions, i.e. tp35, tp55 and tp70, were investigated, but this time, it involved all the case studies in this research.

o get a clearer picture of the effect of every injection position on the $H_m$ as a whole, the number of case studies obtained for each grade was summarized in Table 3. Hence, it was obvious that tp35 had the worst $H_m$ with 13 case studies for Grade B, 14 case studies for Grade C and 1 case study for Grade D. At tp55, 6 case studies were obtained for Grade A, 17 case studies for Grade B while 5 case studies for Grade C. On the other hand, at tp70, 9 case studies were found for Grade A, 12 case studies for Grade B and 7 case studies for Grade C. Although less Grade B and more Grade C were found at tp70 than that at tp55, more Grade A obtained at tp70 made it the optimum injection position which produced the best $H_m$ for all the case studies concerned.

From Table 2, the $M_{hf}$ obtained generally increased with increasing injection positions from the throttle valve, except for a few exceptions observed at tp55 and tp70 ($M_{hf}$ in bold). Nevertheless, owing to the small differences between these $M_{hf}$, the exceptions could be ignored. In other words, the $A/F_m$ was inferior when the injector was positioned further away from the throttle valve. This agreed well with the previous conclusion obtained for a few selected cases.

To sum up, this study yielded the expected results that the $H_m$ was improved while the $A/F_m$ was deteriorated when positioning the injector nearer to the intake manifold. Based on the results obtained for $H_m$, the optimum injection position was tp70. The poor $A/F_m$ at tp70, however, would be treated by an electronic feedback system incorporated with TBIM.

*Table 1 Effect of various injection positions*

| Engine speed (rpm) | Throttle angle (o) | Controlled case tp35 | | Various injection positions tp55 | | tp70 | |
|---|---|---|---|---|---|---|---|
| | | $H_m$ | $M_{hf}$ | $H_m$ | $M_{hf}$ | $H_m$ | $M_{hf}$ |
| 1680 | 30 | C | 0.145 | A | 0.152 | A | 0.191 |
| 2160 | 30 | B | 0.142 | A | 0.155 | A | 0.180 |
| 4500 | 30 | C | 0.072 | B | 0.093 | B | 0.103 |
| 7200 | 30 | C | 0.064 | A | 0.058 | A | 0.079 |

*Table 2 Effect of various injection positions throughout the case studies*

| Engine speed (rpm) | Throttle angle (o) | Various injection positions | | | | | |
|---|---|---|---|---|---|---|---|
| | | tp35 | | tp55 | | tp70 | |
| | | $H_m$ | $M_{hf}$ | $H_m$ | $M_{hf}$ | $H_m$ | $M_{hf}$ |
| 1680 | 0 | C | 0.132 | C | 0.143 | C | 0.150 |
| | 5 | B | 0.124 | B | 0.150 | A | **0.146** |
| | 10 | B | 0.128 | C | 0.144 | B | 0.152 |
| | 15 | B | 0.135 | B | **0.134** | B | 0.165 |
| | 20 | C | 0.143 | B | **0.140** | B | 0.169 |
| | 25 | D | 0.143 | A | 0.154 | A | 0.191 |
| | 30 | C | 0.145 | A | 0.152 | A | 0.191 |
| 2160 | 0 | C | 0.113 | B | 0.125 | B | 0.126 |
| | 5 | C | 0.112 | B | 0.128 | B | **0.122** |
| | 10 | C | 0.115 | B | 0.121 | A | 0.127 |
| | 15 | C | 0.121 | A | 0.134 | A | 0.137 |
| | 20 | C | 0.128 | A | **0.122** | A | 0.145 |
| | 25 | C | 0.092 | B | 0.137 | B | 0.165 |
| | 30 | B | 0.108 | A | 0.155 | A | 0.184 |
| 4500 | 30 | B | 0.072 | B | 0.093 | B | 0.103 |
| | 40 | C | 0.097 | B | **0.090** | A | 0.119 |
| | 50 | C | 0.075 | B | 0.108 | B | 0.122 |
| | 60 | C | 0.081 | B | 0.105 | B | 0.131 |
| | 70 | C | 0.083 | B | 0.109 | B | 0.120 |
| | 80 | C | 0.048 | B | 0.082 | B | 0.112 |
| | 90 | B | 0.034 | B | 0.091 | B | 0.099 |
| 7200 | 30 | B | 0.064 | A | **0.058** | A | 0.079 |
| | 40 | B | 0.057 | B | 0.057 | C | 0.089 |
| | 50 | B | 0.055 | B | 0.065 | C | 0.082 |
| | 60 | B | 0.052 | B | 0.068 | C | 0.082 |
| | 70 | B | 0.051 | C | 0.060 | C | 0.077 |
| | 80 | B | 0.042 | C | 0.072 | C | 0.078 |
| | 90 | B | 0.055 | C | 0.072 | C | 0.080 |

*Table 3 Number of case studies obtained for each grade of $H_m$*

| Injection position | Grades of $H_m$ | | | |
|---|---|---|---|---|
| | A | B | C | D |
| tp35 | | 13 | 14 | 1 |
| tp55 | 6 | 17 | 5 | |
| tp70 | 9 | 12 | 7 | |

## Conclusion

The effect of various injection positions on the $H_m$ and $A/F_m$ in TBIM and intake manifold had been studied in this research. It was found that a varying injection position was incapable to improve the $A/F_m$ but $H_m$ in TBIM and intake manifold. The optimum injection position for $H_m$ throughout the case studies was tp70. The poor $A/F_m$ at tp70, however, would be treated by an electronic feedback system incorporated with TBIM.

## References


[1] Turner, I. ed. 1998. *IMPCO Material Handling & Industrial Engine Gaseous Fuel Training Manual.* Cerritos: IMPCO Technologies, Inc.

[2] Steeg, H. 1990. *Substitute Fuels for Road Transport – A Technology Assessment.* France: International Energy Agency.

[3] Weaver, C. S. 1989. Natural Gas Vehicles – A Review of the State of the Art. *SAE Technical Paper Series.* SAE 892133.

[4] Weider, J. V. D. 2000. Europe's Auto/Oil 2 Program, Understanding the Cost-Benefits of NGVs. *Proceedings of 7th International Conference and Exhibition on Natural Gas Vehicles.* October 17-19. Yokohama, Japan: 67-69.

[5] Gimbres, D., Boree, J., Bazile, R., and Charnay, G. 1999. Effect of Air Pulsed Flow on the Mixture Preparation of Natural Gas SI Engine. *SAE Technical Paper Series.* SAE 1999-01-2905.

[6] Kato, K., Igarashi, K., Masuda, M., Otsubo, K., Yasuda, A. and Takeda, K. 1999. Development of Engine for Natural Gas Vehicle. *SAE Technical Paper Series.* SAE 1999-01-0574.

[7] Dam, W. V., Graham, J. P., Stockwell, R. T. and Montez, A. M. 1998. A New CNG Engine Test for the Evaluation of Natural Gas Engine Oils. *SAE Technical Paper Series.* SAE 981370.

[8] Schafer, F. and Basshuysen, R. V. 1995. Reduced Emissions and Fuel Consumption in Automobile Engines. Germany: Springer-Verlag Wien New York and Society of Automotive Engineers, Inc.

[9] Furuyama, M. and Xu, B. Y. 1998. Mixing Flow Phenomena of Natural Gas and Air in the Mixer of a CNG Vehicle. *SAE Technical Paper Series.* SAE 981391.

[10] Chin, V. D. 2004. Analysis on New Throttle Body Injection System Performance Using Natural Gas for Small Engine. Malaysia: Universiti Teknologi Malaysia: M. Eng. Proposal.

[11] Ouelette, P. and Hill, P. G. 1992. Visualization of Natural Gas Injection for a Compression Ignition Engine. *SAE Technical Paper Series.* SAE 921555.

[12] Klimstra, J. 1989. Carburettors for Gaseous Fuels – On Air-to-Fuel Ratio, Homogeneity and Flow Restriction. *SAE Technical Paper Series.* SAE 892141: 2095-2106.

[13] Tatterson, G. B. 1994. *Scaleup and Design of Industrial Mixing Process.* United States of America: McGraw-Hill, Inc.

[14] Versteeg, H. K. and Malalasekera, W. 1999. *An Introduction to Computational Fluid Dynamics – The Finite Volume Method.* England: Longman Group Ltd.

[15] Anderson, R., Yi, J., Han, Z., Yang, J., Trigui, N., and Boussarsar, R. 2000. Modeling of the Interaction of Intake Flow and Fuel Spray in DISI Engines. *SAE Technical Paper Series.* SAE 2000-01-0656.

[16] Roache, P. J. 1972. *Computational Fluid Dynamics.* Albuquerque: Hermosa Publishers.

[17] Hinz, J. O. 1975. *Turbulence.* New York: McGraw-Hill.

[18] Douglas, J. F., Gasiorek, J. M. and Swaffield, J. A. 1995. *Fluid Mechanics.* 3rd ed. United Kingdom: Longman Scientific and Technical.